

Analyst

Accepted Manuscript



This is an *Accepted Manuscript*, which has been through the Royal Society of Chemistry peer review process and has been accepted for publication.

Accepted Manuscripts are published online shortly after acceptance, before technical editing, formatting and proof reading. Using this free service, authors can make their results available to the community, in citable form, before we publish the edited article. We will replace this *Accepted Manuscript* with the edited and formatted *Advance Article* as soon as it is available.

You can find more information about *Accepted Manuscripts* in the [Information for Authors](#).

Please note that technical editing may introduce minor changes to the text and/or graphics, which may alter content. The journal's standard [Terms & Conditions](#) and the [Ethical guidelines](#) still apply. In no event shall the Royal Society of Chemistry be held responsible for any errors or omissions in this *Accepted Manuscript* or any consequences arising from the use of any information it contains.



Journal Name

ARTICLE

Chromatographic, NMR and vibrational spectroscopic investigations of astaxanthin esters: application to “Astaxanthin-rich shrimp oil” obtained from processing of Nordic shrimps

Received 00th January 20xx,
Accepted 00th January 20xx

DOI: 10.1039/x0xx00000x

www.rsc.org/

B. Subramanian,^{a,b} M.-H. Thibault,^a Y. Djaoued,^{b,*} C. Pelletier,^a M. Touabia,^c N. Tchoukanova^a

Astaxanthin (ASTX) is a keto carotenoid, which possesses a non-polar linear central conjugated chain and polar β -ionone rings with ketone and hydroxyl groups at the extreme ends. It is hailed as a super anti-oxidant, and recent clinical studies have established its nutritional benefits. Although it occurs in several forms, including free molecule, crystalline, aggregates and various geometrical isomers, in nature it exists primarily in the form of esters. Marine animals accumulate ASTX from primary sources such as algae. Nordic shrimps (*P. borealis*), which are harvested widely in the Atlantic ocean, form a major source of astaxanthin esters. “Astaxanthin-rich shrimp oil” was developed as a novel product in a shrimp processing plant in Eastern Canada. A compositional analysis of the shrimp oil was performed, with a view to possibly using it as a nutraceutical product for humans and animals. Astaxanthin-rich shrimp oil contains 50% MUFAs and 22% PUFAs, of which 20% are omega-3. In addition, the Shrimp oil contains interesting amounts of EPA and DHA, with 10%/w and 8%/w, respectively. Astaxanthin concentrations varied between 400 and 1000 ppm, depending on the harvesting season of the shrimp. Astaxanthin and its esters were isolated from the oil and analysed by NMR, FTIR and Micro-Raman spectroscopies. Astaxanthin mono- and diesters were synthesized and used as standards for the analysis of Astaxanthin-rich shrimp oil. NMR and vibrational spectroscopies were successfully used for the rapid characterization of monoesters and diesters of astaxanthin. Raman spectroscopy provided important intermolecular interactions present in the esterified forms of astaxanthin molecules. Also discussed in this paper is the use of NMR, FTIR and Micro-Raman spectroscopies for the detection of astaxanthin esters in shrimp oil.

Introduction

Astaxanthin (ASTX) is a red fat-soluble pigment which has more potent biological activity than other carotenoids.¹ It is of both research and commercial interest due to its well-established antioxidant property. Several excellent reviews discussing the salient features of ASTX and its health benefits to humans have been published,²⁻⁴ and several recent clinical trials of ASTX should be highlighted. In a study on the role of ASTX against obesity, it was found that ASTX normalized the oxidative stress in individuals whose BMI exceeded 25.0 Kg/m².² Park *et al.* demonstrated the protective effect of ASTX towards oxidative DNA damage.⁵ ASTX favorably addressed an aging-induced oxidative attack on red blood cells (RBC) by significantly lowering the RBC hydroperoxide levels.⁶ The

safety and low toxicity of ASTX have been demonstrated in several clinical trials.⁷⁻⁹

ASTX is a very complex molecule (Scheme 1). It consists of two terminal rings joined by a polyene chain. This molecule has two asymmetric carbons located at the 3,3' positions of the β -ionone ring with adjacent ketone (R₂C=O) and hydroxyl (-OH) groups on either end.²⁻⁴ The terminal hydroxyl groups are often found to undergo esterification with saturated fatty acids, monounsaturated fatty acids (MUFAs) or polyunsaturated fatty acids (PUFAs). When one hydroxyl group reacts with a fatty acid it forms a monoester, whereas when both hydroxyl groups are reacted with fatty acids the result is termed a diester. In nature, ASTX is found mostly in esterified forms.

Organisms that synthesize *de novo* ASTX include bacteria, fungi, microalgae and plants.^{1,10} In the microalgae *Haematococcus pluvialis*, ASTX occurs primarily in the form of monoesters (80-94%), with diesters comprising 2-15% and the free molecule 4-5%.¹¹⁻¹³ The predominant fatty acids esters identified are in the C18:n family, with C18:1 being the most abundant.^{12,13} Natural ASTX can also be found in marine animals such as crustacea and salmonid fish, due to accumulation of the pigment in their flesh, and/or shell.^{1,12} The ASTX esters of these secondary sources including shrimps

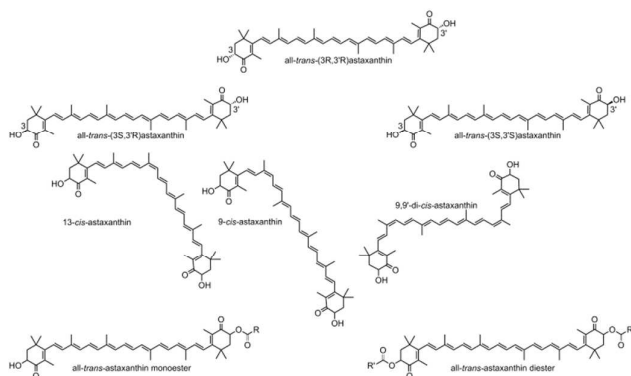
^a Coastal Zones Research Institute, Volet Laboratoires & Services d'Analyses, 232B, rue de l'église, Shippagan, NB, Canada, E8S 1J2.

^b Laboratoire de recherché en matériaux et Micro-spectroscopies Raman et FTIR, Université de Moncton – Campus de Shippagan, NB, Canada, E8S 1P6

^c Département de chimie et biochimie, Université de Moncton, Campus de Moncton, NB, Canada, E1A 3E9.

*Corresponding author: Yahia Djaoued, E-mail: Yahia.djaoued@umoncton.ca

Electronic Supplementary Information (ESI) available: [details of any supplementary information available should be included here]. See DOI: 10.1039/x0xx00000x



(*Pandalus borealis*) and krill (*Euphausia superba*), have been analyzed by various analytical techniques.

Scheme 1 Several structural forms of astaxanthin

In an article by Takaichi *et al.*, free ASTX (20%), ASTX monoesters (34%) and ASTX diesters (46%) were found in krill.¹⁴ In a later study by Grynbaum *et al.*, mono- and di-fatty acid esters of ASTX containing PUFAs such as C20:5 and C22:6 and MUFAs including C18:1 were found in krill.¹⁵ In shrimps (*P. borealis*), Breithaupt has established that the predominant fatty acid esterified with ASTX was C12, and that C18:1 was present both in mono- and diesters.¹³ Renstrom *et al.* have also reported the presence of PUFAs in ASTX esters in *P. borealis*.¹¹ A study on processed shrimp waste by Guillou *et al.*¹⁶ established the ratio of free, mono- and diesterified ASTX to be 5.6%, 18.5 % and 75.9%, respectively. When ASTX esters are consumed by humans or sea animals, their metabolic pathway is closely associated with fatty acids even though they undergo hydrolysis.¹⁷ Furthermore, when their dietary lipid levels were increased, higher levels of ASTX have been deposited and retained in humans and sea animals. Rao *et al.* have shown that when *H. pluvialis* biomass is dispersed in olive oil, the bioavailability and antioxidant properties of ASTX were enhanced in rat plasma and liver tissues; the researchers established that ASTX esters are more protective than free ASTX in UV-7,12 dimethylbenz (a)anthracene (DMBA)-induced skin cancer model in rat.¹⁸ These studies show the importance of ASTX esters in animals and humans. Despite the rapid increase in the studies about the benefits of ASTX for human, it has been acknowledged that the mechanisms that govern increased bioavailability, enhanced antioxidant activity and other metabolic pathways are still unclear. To gain insight on this matter, the first step is to understand the molecular structure of the esters of ASTX. It has to be acknowledged that, in most of the natural sources, ASTX and its esters are only found to be in the range of 100-1000 ppm levels. Hence, it is a serious challenge to obtain molecular information, which is crucial for an understanding of their metabolic activities. Recently, a new product called astaxanthin-rich shrimp oil ('shrimp oil') was developed in the Acadian Peninsula region of New-Brunswick in Canada (patent pending).¹⁹ This shrimp oil, which is rich in omega-3 fatty acids and ASTX, is extracted from the waters used in the processing of shrimp (*P. borealis*), harvested in the coastal zones of Eastern Canada. The 'shrimp

oil' attracted great interest from the market due to its high content in natural ASTX (up to 1000 ppm) and omega-3 fatty acids. The 'shrimp oil' is a complex product, which has several components including fatty acids, triglycerides and carotenoids. Hence, the characterization of shrimp oil poses several challenges.

Given the beneficial effects of ASTX, our focus is on the study of the presence of ASTX and its esters in this new product. Recently we reported the HPLC-HRMS and MS/MS, as well as ¹³C-NMR results concerning the ASTX esters present in the 'shrimp oil'.²⁰ Our objective was achieved by adopting a systematic approach. To begin with, a total fatty acid profile of astaxanthin-rich shrimp oil was obtained. In order to characterize the ASTX and its esters in the astaxanthin-rich shrimp oil, they were extracted using solid phase extraction (SPE). The extract was characterized by HPLC, NMR, FTIR and Raman spectroscopies. To the best of our knowledge, this is the first time that FTIR and Raman spectroscopies are applied to the study of ASTX esters. The HPLC results indicated that, in astaxanthin-rich shrimp oil, ASTX exists predominantly in the form of diesters and monoesters. As it is known that ASTX forms esters of PUFAs, MUFAs, and saturated fatty acids,¹¹⁻¹⁶ we synthesized and isolated mono- and diesters of ASTX following model compounds: (i) ASTX-DHA (ASTX esterified with docosahexaenoic acid (DHA) which is a PUFA) (ii) ASTX-C18:1n-9 (ASTX esterified with *cis*-9-octadecenoic acid (C18:1n-9), a MUFA), and (iii) ASTX-C21 (ASTX esterified with heneicosanoic acid (C21), a saturated fatty acid). Synthesized compounds were characterized by NMR, FTIR, and Raman spectroscopy, thus obtaining their molecular signature. Based on the results obtained from the model compounds, it was possible to analyse the astaxanthin-rich shrimp oil ester extract.

Results and Discussion

Characterization of shrimp oil

Astaxanthin-rich shrimp oil was extracted by centrifugation from the cooking water used during the processing of shrimp (*Pandalus borealis*). Astaxanthin-rich shrimp oil can be described as a dark red, slightly viscous oil with a mild fish odour. The oil was characterized using chromatography, FTIR, Raman and NMR spectroscopies in order to identify its major constituents. Table 1 and table S1 contain characterization data for the shrimp oil. Its distinct red colour indicates the presence of carotenoids which come from the carapaces and tissues of shrimp. The main carotenoid present in shrimp oil is ASTX, as confirmed by HPLC analysis and by comparison with the scientific literature.¹³⁻¹⁶ Total concentrations of ASTX varied from batch to batch and also by harvesting season; they ranged from 400 to 1000 ppm. The different isomers of ASTX and the degree of esterification of ASTX in shrimp oil were determined by HPLC (see experimental section and table 1). The majority of ASTX is in the all-*trans* form. In addition, the molecule exists in two diastereoisomers, (3S,3'R) and (3R,3'R) and one *meso* form (3S,3'R). The ratio of these three

stereoisomers of ASTX found in shrimp oil was evaluated by chiral chromatography and was found to be 30:48:22 for (3*S*,3'*S*), (3*S*,3'*R*) and (3*R*,3'*R*), respectively.

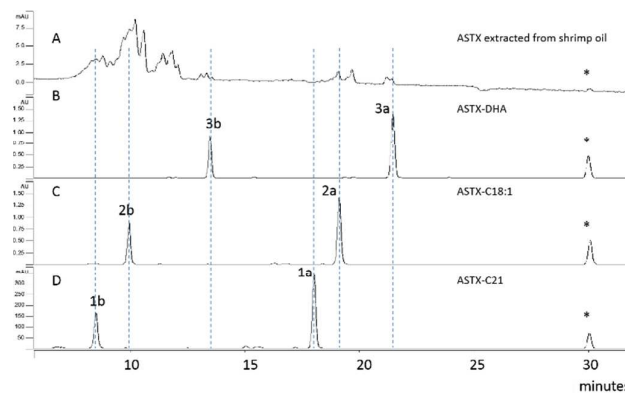
Table 1 Astaxanthin in shrimp oil and general specifications

| Total astaxanthin | 500-1000 µg/g oil |
|--------------------------------|-------------------|
| All- <i>trans</i> -astaxanthin | 57 % |
| 9- <i>cis</i> -astaxanthin | 11 % |
| 13- <i>cis</i> -astaxanthin | 26 % |
| di- <i>cis</i> -astaxanthin | 6 % |
| 3 <i>S</i> ,3' <i>S</i> | 30 % |
| 3 <i>S</i> ,3' <i>R</i> | 48 % |
| 3 <i>R</i> ,3' <i>R</i> | 22 % |
| Diesters | 75 % |
| Monoesters | 23 % |
| Free (diol) | 2 % |
| Fat | ~ 100 % |
| Sterols | 1.7 % |
| Cholesterol | 0.8 % |
| Triglycerides | >95 % |
| Fatty acids | 87 % |
| Saturated | 18 % |
| Monounsaturated | 46 % |
| Polyunsaturated | 23 % |
| Vitamin A | 1483 RE/100g |
| Vitamin E | 43 mg/100g |

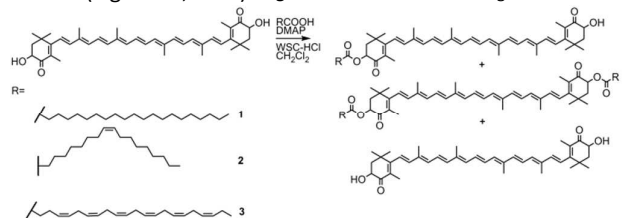
Finally, in shrimp oil, ASTX is close to 100% esterified and found in the form of diesters at 75%. This result is consistent with other studies on shrimp products by Breithaupt¹³ and Guillou.¹⁶ Table 1 shows that shrimp oil is constituted of fat, of which more than 95% is in the form of triglycerides. The remaining 5% are sterols and unidentified fatty acids. The cholesterol (0.8%) may undergo auto-oxidation and photo-oxidation, as both processes give rise to oxysterols of various structures depending on the type of oxidation and the physical state of the substrate. The sterols, including the cholesterol, its precursors such as 7-dehydrocholesterol, and its harmful oxidation products are currently under investigation. Total fatty acid profile analysis (table S1) reveals that almost 50% are monounsaturated fatty acids, 22% are polyunsaturated and 20% are omega-3 acids. Shrimp oil contains interesting amounts of EPA and DHA, with 10%/w and 8%/w, respectively.

Chromatography

Figure 1 A shows the chromatogram at 478 nm of an ASTX fraction extracted from shrimp oil and ran under normal phase conditions. Two areas representing the ASTX-esters are recognizable in the chromatogram. The peaks between 7 and 12 minutes and those between 17 and 22 minutes are attributed to ASTX-diester and ASTX-monoesters, respectively. Based on the types of fatty acids found in the shrimp oil (table S1), we synthesized ASTX-esters with saturated, monounsaturated and polyunsaturated fatty acids to be used as standards for analysis by vibrational and NMR spectroscopies. ASTX was esterified according to a method reported by Fukami et al.²¹ Esterification was performed with



heneicosanoic acid (C21)(**1**), 9-octadecenoic acid (C18:1n-9)(**2**) and docosahexaenoic acid (DHA, C22:6n-3)(**3**) and afforded the mono- (**a**) and the diester (**b**) as well as some unreacted free ASTX (scheme 2). The chromatograms of the synthesized ASTX esters (Figure 1, B-D) Fig. 1 HPLC-DAD chromatograms from the



synthesized astaxanthin-esters compared to ASTX extracted from shrimp oil. * free astaxanthin

Scheme 2 Synthesis of astaxanthin mono- (**a**) and diesters (**b**)

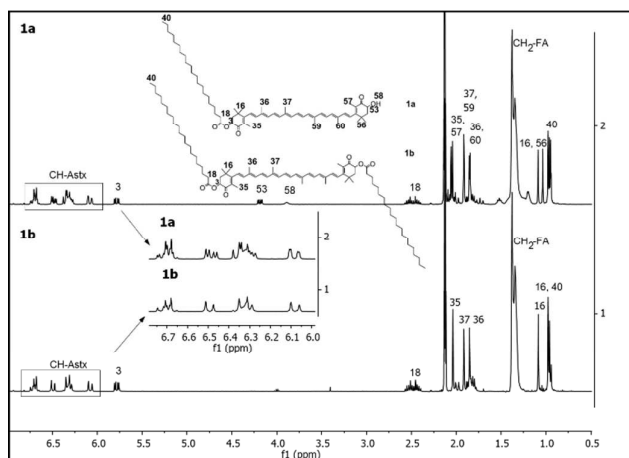
were compared to the chromatogram of ASTX extracted from shrimp oil. It is clearly seen that each type of ASTX esters present in shrimp oil is represented. The order of elution of the ASTX species described above has been validated using the synthetic ASTX-esters. The retention times were also dependent on the degree of saturation of the fatty acid ester: saturated ASTX-C21 esters came out first, then the monounsaturated ASTX-C18:1n-9 and finally the polyunsaturated ASTX-DHA.

Analysis of synthetic astaxanthin esters

The synthetic ASTX esters were separated on a silica column and analysed by NMR spectroscopy, FTIR and Raman spectroscopies.

NMR

Figure 2 shows the ¹H NMR spectra of **1a** and **1b**. In all cases, signals between 6.0 and 7.0 ppm represent the methine protons on the ASTX backbone. These signals appear as two sets in the monoesterified compounds due to the loss of symmetry (see inset in figure 2). Let us first examine the ¹H NMR spectrum of ASTX-C21 diester **1b**. In the spectrum, a doublet of doublet integrating for two protons (*J* = 14.1, 5.3 Hz) at 5.78 ppm represents the proton on the asymmetric carbons #3,3' (figure 2). At 2.47 ppm, a multiplet integrating for four protons corresponds to the methylene protons α to the carbonyl (#18). Singlets at 2.04, 1.92 and 1.82 ppm,



correspond to the methyl moieties #35, #37 and #36, respectively. The two methyl groups on the β -ionone ring come out at 1.09 and 0.92 ppm. A large signal corresponding to the methylene protons on the fatty acid moiety appears between 1.25 and 1.4 ppm. Overlapping peaks

Fig. 2 ^1H NMR spectra of ASTX-C21 mono- (**1a**) and diester (**1b**)

appearing around 1.85 and 2.0 ppm correspond to the methylene protons #19 and #2. A triplet ($J = 7.1$ Hz) at 0.96 ppm is attributed to the methyl end group on the fatty acid moiety. The ^1H NMR of **1a** is similar to **1b**. However, the presence of a doublet of doublet ($J = 13.8, 5.7$ Hz) at 4.19 ppm and at 5.78 ppm both integrating for one proton, indicates a loss of symmetry due to the presence of only one fatty acid moiety. Moreover, a broad signal at 3.89 ppm corresponds to the OH moiety on the ASTX molecule. The methine signals appear as two sets, another indication of a monoesterified ASTX molecule. In the same line of thought, the methyl groups on the ASTX backbone appear as singlets at 2.06, 2.04, 1.91, 1.85, 1.84, 1.09, 1.04, 0.98 and 0.95 ppm. Similar observations can be made for **2a**, **2b** (Figure S1) and **3a**, **3b** (Figure S2). In addition, the presence of unsaturated fatty acids is detectable by the appearance of multiplets between 5.2–5.4 ppm attributed to methine protons. In all cases, the integrations in the proton spectra were challenging, particularly when comparing signals coming from the ASTX backbone and the fatty acids moieties. This was especially apparent for compounds **3a** and **3b**. Interestingly, it has been reported by Kobayashi *et al.* that some unsaturated fatty acids have long spin-lattice (T_1) constants, reaching 3.5 s for the methylene protons on DHA in CDCl_3 .²² Longer T_1 can prevent the nuclear spin to reach thermal equilibrium before being probed, which can lead to loss of quantitative signal for the protons involved. This may explain the difficulties encountered in the integration of the proton spectra. In the $^{13}\text{C}\{^1\text{H}\}$ NMR spectra, the signals attributed to the carbon atoms found in the carbonyl moieties are good indicators of a mono- or diesterified ASTX. Diesterified ASTX has two kinds of carbonyl groups; one on the ionone ring and one on the esters. For compound **1b**, the carbonyl on the β -ionone ring comes out at 193 ppm whereas

the carbonyl signal arising from the ester moiety is situated upfield at 172 ppm. In the case of the monoester **1a**, three types of carbonyl signals are expected; one from the ester moiety, one from the ionone ring bonded to the ester and one from the ionone ring that is not esterified. The latter is situated downfield from the esterified carbonyl at 200 ppm while the other two come out at the same chemical shifts as the diesterified ASTX (Figure S3).

FTIR

Figure S4 (A, B, C and D) shows FTIR spectra of ASTX, C21, C18:1n-9 and DHA fatty acids respectively, and allow a better understanding of the FTIR spectra of ASTX-esters. In Figure S4A, the FTIR spectrum of ASTX, the signature mode is seen at 1651.8 cm^{-1} , which arises due to the $\text{C}=\text{O}$ groups present in the terminal β -ionone rings.^{23,24} The hydroxyl group shows a peak at 3484.8 cm^{-1} . $\text{C}=\text{C}$ stretching vibrations of conjugated structures $\text{C}=\text{C}$, is seen at 1548.6 cm^{-1} . FTIR spectroscopy is sensitive to the $\text{C}-\text{C}$ stretching vibrations of the central conjugated structure of ASTX and is observed as a broad band. This band is composed of three absorption peaks with frequencies of $975.8, 962.3,$ and 953.6 cm^{-1} . In addition to those mentioned above, several other peaks with relatively lower intensities are seen which are assigned and listed in supplementary information.^{25,26} Table S2 shows FTIR bands and assignments for C18:1n-9, C21 and DHA fatty acids. According to Yoshida *et al.*, the CH stretching of alkene group ($\text{HC}=\text{CH}$) observed at $\sim 3008\text{ cm}^{-1}$, was used to quantify the presence of unsaturated bonds.²⁷ In the case of C21, such a peak is not observed. In the case of C18:1n-9, a peak at 3008.5 cm^{-1} is seen with small absorption whereas DHA shows a high intense absorption peak at 3013.3 cm^{-1} . This observation is in accordance with the nature of fatty acids used in this work: C21 is a saturated fatty acid, C18:1n-9 is monounsaturated fatty acid and DHA is polyunsaturated fatty acid. The esterification reaction is a result of a condensation reaction occurring between the carboxyl group of the fatty acid and one of the two hydroxyl groups of ASTX, forming a $\text{C}-\text{O}-\text{C}$ bond. In the case of monoesters such reaction will happen only on one side of the ASTX molecule, whereas the $-\text{OH}$ on the other end remains intact. Hence to infer about the ester it is instructive to look at the FTIR modes due to OH, $\text{C}=\text{O}$, and $\text{C}-\text{O}-\text{C}$ bonds. With this general idea, FTIR spectrum of ASTX-monoesters are examined. Figure 3A shows the FTIR spectra of ASTX-C21 monoester **1a**.

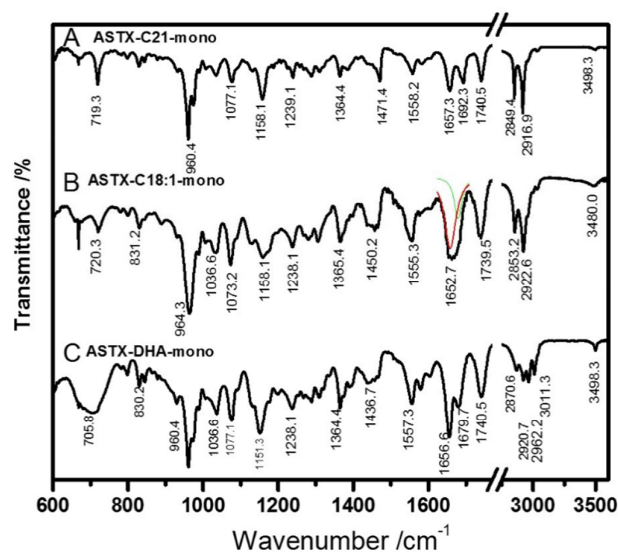


Fig. 3 FTIR spectra of ASTX-C21 monoester (**1a**), ASTX-C18:1n-9 monoester (**2a**), and ASTX-DHA monoester (**3a**)

The spectrum shows a mode at 3498.3 cm^{-1} , which emerges from the stretching vibrations of the free OH of the ASTX molecule **1a**. The intensity of OH bands is approximately reduced by half when compared with the intensity of OH bands of free ASTX molecules. Interesting modifications are seen in the FTIR mode of C=O bonds present in **1a** as compared to free ASTX. The formation of C=O bonds in esters is evidenced by the presence of the 1740.5 cm^{-1} mode, which is a signature mode for ester group. The bands seen at 1657.3 and 1692.3 cm^{-1} are emerging from stretching vibrations of ketonic C=O bonds of ASTX (β -ionone rings). Two kinds of vibrations of ketonic C=O of ASTX can be explained as follows. The vibrational mode seen at 1657 cm^{-1} is similar to free ASTX, from the non-esterified end. The environment of ketone group in the esterified end is significantly changed, in such a way that more energy is required for the C=O stretching vibration due to the binding of fatty acid. This leads to a blue shift in the ketonic C=O bond present in the esterified end of ASTX and appears at 1692.3 cm^{-1} . The peak at 1158.1 cm^{-1} is assigned to the C-O-C stretching. Thus, the esterification leads to comprehensive changes in the OH, C=O and C-O-C stretching bands seen in the FTIR spectrum, when compared to free ASTX and C21 fatty acid figures S4A and S4B. Figure 3B shows the FTIR spectrum of ASTX-C18:1n-9 monoester **2a**. Similar to **1a**, the hydroxyl group is present at 3480.0 cm^{-1} , but with reduced intensity compared to that of free ASTX. The signature ester mode due to C=O is seen at 1739.5 cm^{-1} . The stretching vibrations of ketonic C=O bonds exhibit overlap of two bands seen at 1679.2 and 1657.9 cm^{-1} . These two modes confirm the formation of a monoester as discussed earlier for **1a**. The stretching modes of C-O-C bonds are seen at 1158.1 cm^{-1} . Figure 3C shows the FTIR spectrum of ASTX-DHA monoester **3a**. The hydroxyl group of **3a** is seen at 3498.3 cm^{-1} , similar to the ASTX-monoesters discussed above. The characteristic C=O ester mode is seen at 1740.5 cm^{-1} . Splitting of C=O mode is also seen in the case of **3a** as a peak at 1656.6 and a shoulder

at 1679.7 cm^{-1} characteristic of a monoester. The C-O-C mode is seen at 1151.3 cm^{-1} . In addition to this, the relatively strong mode at 3011.3 cm^{-1} shows the presence of polyunsaturated fatty acid. From the above results, signature modes of ASTX-monoesters were defined for their FTIR spectra.

Figure 4 (A, B and C), shows the FTIR spectra of ASTX-C21 diester (**1b**), ASTX-C18:1n-9 diester (**2b**) and ASTX-DHA diester (**3b**), respectively. In ASTX diesters, C-O-C bonds form on both end of the ASTX molecule. In the case of **1b**, the signature ester band is observed at 1744.3 cm^{-1} . The mode due to C=O bond in the β -ionone ring is seen at 1674.9 cm^{-1} . The OH band is absent in the case of **1b**. The mode due to C-O-C bond is seen at 1159.0 cm^{-1} . The absence of OH band clearly suggests that the esterification is complete on either end of the ASTX molecule. Interestingly, as the stretching vibration of ketonic C=O is under the influence of the fatty acid environment on either end of ASTX molecule, only one mode in the FTIR spectrum is seen at 1674.9 cm^{-1} , instead of two modes seen with **1a** (Figure 3A). This observation can also be considered as the signature for the formation of a diester.

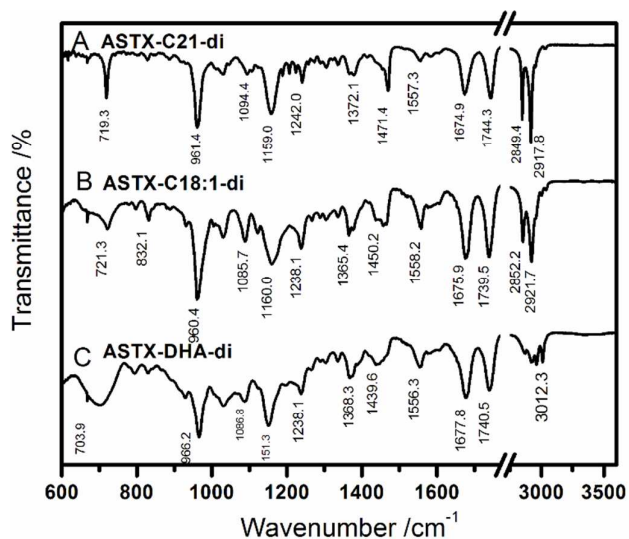


Fig. 4 FTIR spectra of ASTX-C21 diester (**1b**), ASTX-C18:1n-9 diester (**2b**), and ASTX-DHA diester (**3b**)

The C-O-C band is seen at 1159.0 cm^{-1} . The intensity of this band is found to be higher in these spectra when compared to that of ASTX-C21 monoester. This increase in intensity is attributed to the population of C-O-C bonds which are twice in number compared to that of monoester. Similarly to **1b**, the FTIR spectra of **2b**, and **3b** show absence of bands for the OH group. The FTIR mode due to C=O ester group is observed at 1739.5 and 1740.5 cm^{-1} in **2b** and **3b** respectively. The ketonic C=O shows only one mode for **2b** and **3b**, evidencing the formation of diesters. Similar to **1b**, **2b** and **3b** show bands at 1160.0 and 1151.3 cm^{-1} , due to C-O-C stretching. Thus, monoesters and diesters of ASTX could be clearly and precisely identified by FTIR spectroscopy.

Raman

Raman spectroscopy can distinguish two types of organic molecular crystals of ASTX, identified as type A and type B.^{25,26}

Their Raman spectra are presented in Figure S5. The spectra are normalized and compared to each other in the spectral range where their distinguishable features are seen. It may also be noted that the type A crystal structure is the result of π -stacking interaction and type B structure is the result of head to tail interaction.

Figure 5 (A, B and C) shows the Raman spectra of ASTX-monoesters **1a**, **2a** and **3a**, respectively, in the range of 100 to 4000 cm^{-1} . The spectra presented in Figure 5 are compromised for intensity. The Raman spectra of ASTX-monoesters show a mode at 1650.7 cm^{-1} , which belongs to the C=O mode of the ketonic group of ASTX. The intensity of this mode is half when compared to that of pure ASTX. This indicates that the formation of monoesters causes the local environment changes. In the case of monoesters, one side is not esterified hence the Raman spectra from the C=O end of non-esterified can still be seen as a faint peak at 1650 cm^{-1} . In addition to this peak, one can see the presence of a new mode at 1680 cm^{-1} ,

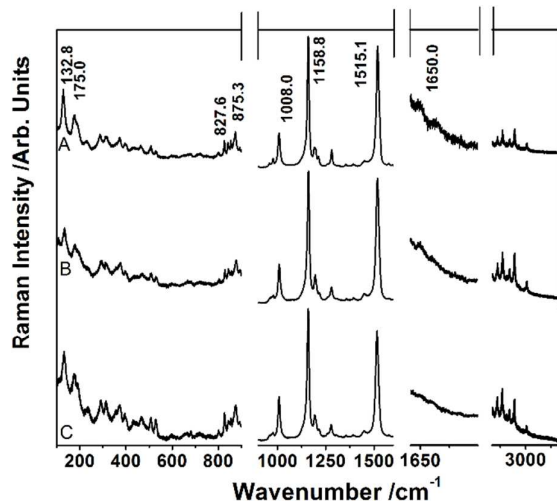


Fig. 5 Raman spectra of ASTX-C21 monoester (**1a**), ASTX- C18:1n-9 monoester (**2a**), and ASTX-DHA monoester (**3a**)

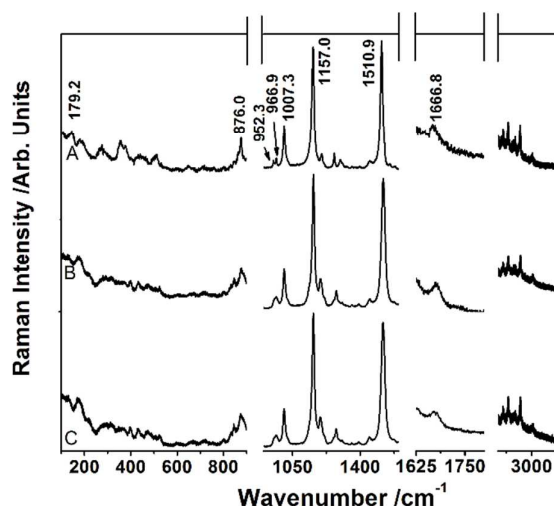


Fig. 6 Raman spectra of ASTX-C21 diester (**1b**), ASTX- C18:1n-9 diester (**2b**), and ASTX-DHA diester (**3b**)

which is assigned to the stretching vibration of C=O from the ketone on the esterified end. In the spectral region below 200 cm^{-1} , modes seen at 128.6, and 177.2 cm^{-1} are similar to that of type B crystal structure, which is formed due to the head to tail interaction. Furthermore, Raman modes between the wavenumbers 800 and 1000 cm^{-1} are exceptionally similar to that of type B crystal structure as all the monoesters show peaks at 800, 825, 840, 853, 875, 958, and 976 cm^{-1} . Hence, it is evident that an intermolecular interaction is occurring in the case of ASTX monoesters through the formation of head to tail bonding between non esterified ends of the monoesters.

Figure 6A, B and C shows Raman spectra of ASTX diesters **1b**, **2b** and **3b**, respectively. In contrast with the monoesters, the ketonic C=O is seen at a higher wavenumber, in the range of 1667 to 1679 cm^{-1} , with higher intensity. This clearly evidences that monoesters and diesters could be identified from the peak shifts and intensity of ketonic C=O of ASTX. Furthermore, the Raman modes below 200 cm^{-1} and in the interval of 800-1000 cm^{-1} are similar to that of type A crystal structures of pure ASTX. Type A crystal structure is formed when the π -stacking interaction occurs in the conjugated structure of ASTX part of the diesters. It is remarkably the only possibility in diesters, as either end is completely esterified. Hence this observation evidences that π -stacking intermolecular interaction is observed in the ASTX diesters.

Analysis of Shrimp oil

Based on the previous investigation of synthetic ASTX esters, astaxanthin-rich shrimp oil is analysed. Shrimp oil contains several compounds of biological importance including omega-3 fatty acids and ASTX. In general, ASTX is present at $\sim 0.1\%$ in shrimp oil. In order to increase the concentration of ASTX for the purpose of analysis and identification, ASTX related compounds (Eg: ASTX esters and free ASTX) were extracted from the shrimp oil by SPE. In this process, shrimp oil without ASTX was also obtained. Fatty acid profile of the ASTX-extract (data not presented) shows that the fraction containing ASTX

is enriched in polyunsaturated fatty acids in regards to the whole shrimp oil. It should be mentioned that the extract still contains mostly triglycerides and ASTX represents less than 1 % of its mass. Figure 7 shows the NMR spectra of shrimp oil, ASTX-extract and ASTX-DHA diester (**3b**). The NMR spectrum of shrimp oil resembles those of oils containing mainly triglycerides and assignment of the peaks was done by comparison with the literature (table S5).²⁸⁻³⁰ Signals attributed to protons on PUFAs (0.96, #9; 2.09 ppm, #5), DHA (2.39 ppm, #3) and EPA (1.69 ppm, #7) are easily seen on the spectra of shrimp oil and of the ASTX-extract. Integration of these signals shows an increase in PUFAs content in the ASTX-extract compared to the shrimp oil, as was also observed in the total fatty acid profile of the extract. The concentration in ASTX and its esters in the shrimp oil is too low to be detected by NMR. Comparison of NMR spectra of **3d** and ASTX-extract shows that while some signals are very similar between ASTX-DHA and DHA (#9), others have different chemical shifts (#3).

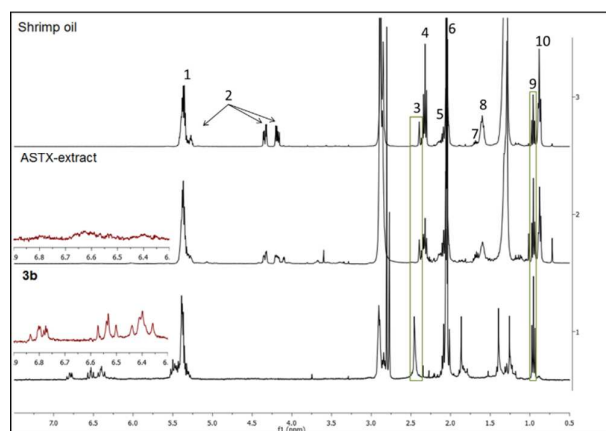


Fig. 7 ¹H NMR spectra of shrimp oil, ASTX-extract and ASTX-DHA diester (**3b**). Assignations of the signals are given in table S5.

This could allow differentiation between DHA-triglyceride and ASTX-DHA, and eventually between ASTX-EPA and EPA-triglyceride.

ASTX-extract and ASTX-free shrimp oil were also studied by vibrational spectroscopies. The previous sections demonstrated that FTIR modes due to OH, C=O and C-O-C bonds constitute the signature modes of ASTX esters which occur in the spectral regions of 3300-3500, 1630-1660, and 1660-1900 cm^{-1} , respectively. Figure 8 shows the FTIR spectra of ASTX-extract, astaxanthin-free shrimp oil and ASTX-DHA. Signature regions (spectral regions of 2750-4000 and 1500-1850 cm^{-1}) are enlarged and presented as insets in Figure 8. The signature mode of ASTX is located at 960 cm^{-1} , which is evident in the pure ASTX-DHA diester spectrum, and in proportion to it, the intensity of the ester mode is seen at 1740 cm^{-1} . A signal of very small intensity is seen at 960 cm^{-1} for the signature mode of ASTX in the case of ASTX extract. Proportionately, a small intensity is anticipated at 1740 cm^{-1} . Instead, a broad band with higher intensity is observed at 1743 cm^{-1} , with a shoulder on the lower wavenumber side. In order

to understand the differences in wavenumber and in intensity of the band attributed to carbonyl esters around 1740 cm^{-1} , a comparison with the FTIR spectrum of ASTX-free shrimp oil was made. This spectrum shows a narrow band at 1740 cm^{-1} owing to the ester bonds of triglycerides. In the FTIR spectrum of ASTX-extract, which also contains triglycerides, the band at 1740 cm^{-1} can be attributed to the ester bonds of triglycerides. An important difference between the ester bands is the extra shoulder seen in the case of ASTX-extract. This shoulder can be a result of the contribution of ASTX-esters and PUFAs. This assignment gets support from the pure ASTX-DHA ester spectrum, which also shows a similar band. Furthermore, the ASTX-extract shows a higher intensity PUFA signature band compared to that of ASTX-free shrimp oil, indicating that ASTX-extract is richer in PUFA (Figure 8: Inset-2). A striking similarity between ASTX extract and ASTX-DHA ester is seen through the broad band at 3400 cm^{-1} (Inset-2). This band is not seen in the case of ASTX-free shrimp oil or in the case of ASTX-C21 diesters (it can be seen with the C18:1 diester). This suggests that the ASTX extract may contain ASTX-PUFA and MUFA esters. Figure S6 shows the Raman spectra of the ASTX extract and ASTX-free shrimp oil. In the 1600-1700 cm^{-1} spectral region, a peak at 1650 cm^{-1} is seen in the Raman spectrum of ASTX-free shrimp oil. In the case of ASTX extract, signature modes for ASTX are seen at 1157 and 1521.6 cm^{-1} . Also, a relatively broader peak is seen at 1650 cm^{-1} , which upon deconvolution shows a low intensity peak at 1670 cm^{-1} along with 1650 cm^{-1} . The peak at 1670 cm^{-1} , is attributed to the C=O of ketone group of ASTX-diester, following the Raman analysis of synthesized ASTX-diester (Figure 6). The peak seen at 1650 cm^{-1} is attributed to the C=C of fatty acids present in the triglycerides of shrimp oil. In order to show the capability of Raman spectroscopy in detecting ASTX directly in Astaxanthin-rich shrimp oil matrices, three shrimp oil samples having different ASTX concentrations were analysed. Figure 9 shows the Raman spectra of shrimp oil with ASTX of concentrations 0, 283, and 893 ppm along with their white light optical microscope images. The intensity of signature modes for

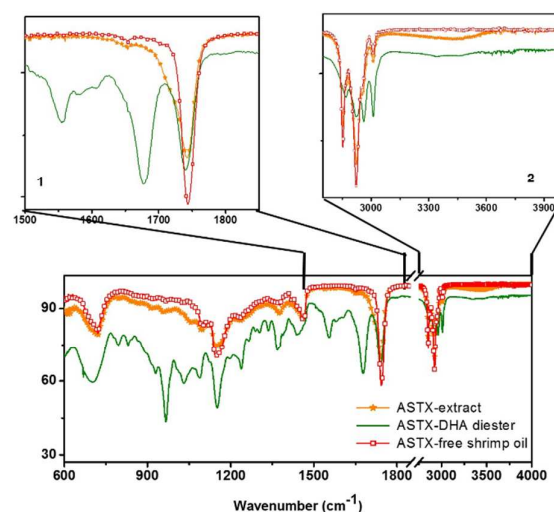


Fig. 8 FTIR spectrum of astaxanthin extract of shrimp oil and ASTX-free shrimp oil.

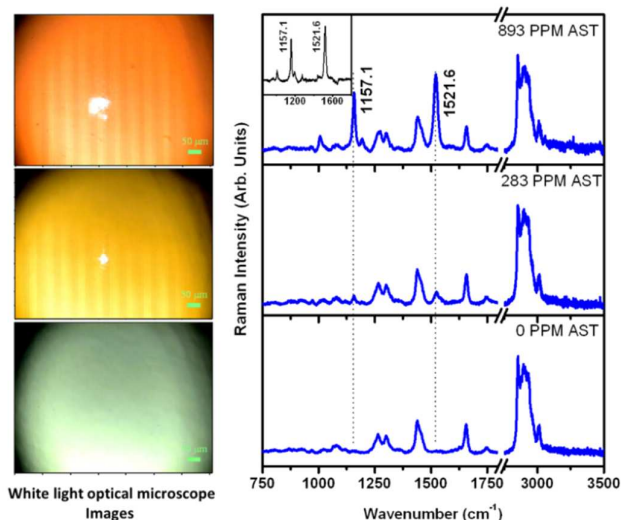


Fig. 9 Raman spectra of ASTX free shrimp oil and with ASTX of concentrations 283, and 893 ppm and their white light optical images. Colours in optical images vary according to the ASTX concentration.

ASTX at 1157 and 1521.6 cm^{-1} varies monotonically with the concentration of ASTX present in shrimp oil, facilitating the identification of ASTX in ppm level.

Experimental

Materials

Astaxanthin was purchased from Sigma-Aldrich and Alexis Biochemicals and stored under nitrogen at $-20\text{ }^{\circ}\text{C}$. Solvents were purchased from Fisher Scientific and used as received except dichloromethane (DCM), which was dried with molecular sieves (4 Å). 4-(dimethylamino)pyridine (DMAP) and [3-(dimethylamino)propyl]-3-ethylcarbodiimide hydrochloride (WSC·HCl) were purchased from Sigma-Aldrich and used as received. 9-octadecenoic acid (C18:1n-9), heneicosanoic acid (C21:0) and 4,7,10,13,16,19-docosahexaenoic acid (C22:6n-3) were purchased from Nu-Chek Prep Inc. and used as received. Butylated hydroxytoluene (BHT) was purchased from VWR and used as received. Acetone- d_6 and toluene- d_8 were purchased from Sigma-Aldrich and used as received.

Shrimp oil was produced and provided by the Island Fishermen Cooperative Association LTD (Lamèque, NB, Canada). The shrimp oil is obtained as a byproduct from Northern shrimp processing facilities. Particularly, shrimp processing water is recovered and subjected to a dissolved air flotation system after adding a flocculating agent. The suspended and dissolved solids form aggregates that are recovered from the surface by means of a procedure referred to as "skimming". The skimming product is then directed into a horizontal centrifuge (settling tank) in order to separate the solid phase (SOC) and the liquid phase consisting of water and shrimp oil. The liquid phase is pumped into the 3-phase vertical centrifuge in order to separate the shrimp oil, the water, and the solids. The resulting shrimp oil is very rich in astaxanthin

and in long-chained omega-3 fatty acids. It has a bright red color attributed to the presence of astaxanthin (Figure S7).¹⁹ In order to avoid oxidation process, the shrimp oil was kept under N_2 and stored at low temperature in the dark.

The analytical stationary phase (Luna Silica 3 μm 4.6 x 150 mm) was purchased from Phenomenex (Torrance, CA, USA). The analytical stationary phase Chirapack IC 5 μm 4.6 x 250 mm was purchased from Canadian Life Science. The GC capillary column ZB-Wax 20m x 0.18 mm x 0.18 μm was purchased from Phenomenex.

Extraction of astaxanthin from shrimp oil

Samples for HPLC were prepared by first extracting the ASTX from the shrimp oil using solid phase extraction (SPE). When needed a saponification step was added after the extraction. The complete extraction and saponification method is given in the supporting information.

Synthesis of astaxanthin esters

All esterification reactions were carried out using the same method and work-up.

Astaxanthin (30 mg, 0.05 mmol), heneicosanoic acid (19.4 mg, 0.06 mmol) or *cis*-9-octadecenoic acid (15.5 mg, 0.055 mmol) or docosahexaenoic acid (18.1 mg, 0.055 mmol), DMAP (3.3 mg 0.03 mmol) and (WSC·HCl) (14.6 mg, 0.08 mmol) were dissolved in 4 mL DCM and flushed with nitrogen. The solution was stirred at room temperature for 18h, after which 15 mL DCM were added. The mixture was then washed with 3 mL each of HCl 1 M, and saturated solutions of sodium carbonate and sodium chloride. The organic phase was separated and dried over a column (15 g) of sodium sulphate. The solvent was evaporated under a flow of nitrogen to leave a dark red solid.

ASTX-C21: The diesters, monoesters and remaining free astaxanthin were separated by silica gel column chromatography (10 g, hexanes:ethyl acetate) increasing the solvent polarity from 1:0 to 7:3 (v/v). **ASTX-C21-diester (1b)** came out first as a dark red oily compound. ^1H NMR (400 MHz, Toluene- d_8) δ 6.71 (m, 4H), 6.49 (d, J = 14.8 Hz, 6H), 6.31 (m, 6H), 6.08 (d, J = 16.1 Hz, 2H), 5.78 (dd, J = 14.1, 5.3 Hz, 2H), 2.47 (ddt, J = 30.5, 15.5, 7.7 Hz, 4H), 2.04 (s, 6H), 1.99 (m, 2H), 1.92 (s, 6H), 1.90-1.77 (m, 6H), 1.85 (s, 6H), 1.40-1.26 (br, 68H), 1.09 (s, 6H), 0.98 (s, 6H), 0.96 (t, J = 6.8 Hz, 6H) ppm. ^{13}C NMR (101 MHz, Toluene- d_8) δ 192.67, 172.08, 158.59, 141.63, 139.55, 136.43, 134.82, 134.36, 133.96, 130.76, 124.18, 123.30, 70.52, 42.72, 36.61, 34.19, 32.07, 30.0-29.9 (br), 29.88, 29.74, 29.57, 29.55, 29.27, 25.66, 25.19, 22.82, 14.01, 13.99, 12.40, 12.05 ppm. **ASTX-C21-monoester (1a)** came out second also as a dark red oily solid. ^1H NMR (400 MHz, Toluene- d_8) δ 6.71 (m, 4H) 6.51 (d, J = 15.2 Hz, 1H), 6.46 (d, J = 15.0 Hz, 1H), 6.35 (m, 6H), 6.09 (d, J = 16.3 Hz, 1H), 6.08 (d, J = 16.4 Hz, 1H) 5.78 (dd, J = 14.3, 5.5 Hz, 1H), 4.19 (dd, J = 13.7, 5.8 Hz, 1H), 3.89 (br, 1H), 2.47 (ddt, J = 30.45, 15.45, 7.64 Hz, 2H), 2.07 (m, 2H), 2.06 (s, 3H) 2.04 (s, 3H), 1.99 (m, 2H), 1.91 (s, 6H), 1.85 (s, 3H), 1.84 (s, 3H), 1.82 (m 2H), 1.40-1.30 (br, 46H) 1.09 (s, 3H), 1.04 (s, 3H), 0.98 (s, 3H), 0.96 (t, J = 7.1 Hz, 3H), 0.95 (s, 3H).

ASTX-C18(1): The diesters, monoesters and remaining free astaxanthin were separated by silica gel column chromatography (10 g, hexanes:ethyl acetate) increasing the solvent polarity from 1:0 to 7:3 (v/v). **ASTX-C18(1)-diester (2b)** came out first as a dark red compound. ^1H NMR (400 MHz, Acetone- d_6) δ 6.81 (m, 4H), 6.55 (m, 4H), 6.42 (m, 6H), 5.51 (m, 2H), 5.38 (m, 4H), 2.40 (m, 4H), 2.07-2.04 (m, 15H), 2.03 (s, 6H), 1.88 (s, 6H), 1.68 (p, $J = 7.6$ Hz, 4H), 1.41 (s, 12H), 1.40-1.29 (36 H), 1.28 (s, 6H), 0.90 (brt, $J = 6.8$ Hz, 6H) ppm. ^{13}C NMR (101 MHz, Acetone- d_6) δ 193.2, 172.0, 160.3, 142.0, 139.5, 136.7, 134.9, 134.9, 133.8, 130.8, 129.7, 129.7, 127.7, 125.0, 123.5, 70.5, 42.5, 36.9, 33.7, 31.7, 29.8, 29.6, 29.0, 28.9, 28.8, 26.9, 26.9, 25.6, 24.8, 22.4, 13.5, 13.4, 11.9, 11.7 ppm there are four signals which are overlapping with the acetone- d_6 signal at 28.9 ppm, as seen from the hsqc spectrum. **ASTX-C18(1)-monoester (2a)** came out second also as a dark red solid. ^1H NMR (400 MHz, Acetone) δ 6.80 (m), 6.54 (m), 6.41 (m), 5.51 (m), 5.38 (m, 2H), 4.30 (m, 1H), 3.95 (br d, $J = 2.4$ Hz, 1H), 2.40 (m, 2H), 2.03 (s, 1H), 1.90 (s, 1H), 1.88 (s, 1H), 1.68 (m, 2H), 1.41 (s, 1H), 1.37-1.31 (br, 20H), 1.28 (s, 3H), 1.23 (s, 3H), 0.90 (t, $J = 6.8$ Hz, 3H).

ASTX-DHA: The diesters, monoesters and remaining free astaxanthin were separated on silica gel column chromatography (10 g, hexanes:ethyl acetate) slowly increasing the solvent polarity from 1:0 to 7:3 (v/v). **ASTX-DHA-diester (3b)** came out first as a dark red oily compound. ^1H NMR (400 MHz, Acetone- d_6) δ 6.88 – 6.74 (m, 4H), 6.62 – 6.49 (m, 5H), 6.48 – 6.33 (m, 6H), 5.59 – 5.42 (m, 20H), 5.44 – 5.28 (m, 22H), 2.90 – 2.82 (m, 9H), 2.50 – 2.43 (m, 40H), 2.03 (s, 9H), 1.88 (s, 6H), 1.87 – 1.78 (m, 2H), 1.41 (s, 10H), 1.28 (s, 9H), 1.35 – 1.17 (m, 6H), 0.97 (t, $J = 7.5$ Hz, 20H), 2.98 – 2.88 (m, 42H). **ASTX-DHA-monoester (3a)** came out second as a dark red oily compound. ^1H NMR (400 MHz, Acetone- d_6) δ 6.89 – 6.70 (m, 3H), 6.62 – 6.48 (m, 3H), 6.41 (td, $J = 15.5, 14.6, 6.6$ Hz, 5H), 5.59 – 5.47 (m, 1H), 5.46 – 5.24 (m, 7H), 4.37 – 4.21 (m, 1H), 3.95 (d, $J = 2.5$ Hz, 0H), 2.92 (dd, $J = 7.5, 4.2$ Hz, 5H), 2.88 – 2.84 (m, 4H), 2.47 (h, $J = 3.0, 2.4$ Hz, 3H), 2.03 (s, 4H), 1.91 (s, 2H), 1.88 (s, 2H), 1.87 – 1.71 (m, 3H), 1.42 (s, 2H), 1.37 (s, 2H), 1.46 – 1.19 (m, 2H), 1.28 (s, 2H), 1.23 (s, 2H), 0.97 (t, $J = 7.5$ Hz, 3H).

Chromatography

The analytical separations were performed on a Varian ProStar HPLC system with quaternary pump (ProStar 240), an autosampler (ProStar 410), a degasser (MicroSolv Technology Corporation, Eatontown NJ, USA) and using a ProStar 335 photodiode array detector (PAD). Data was processed using Varian Star Workstation.

Total astaxanthin analyses were performed using a normal phase Luna Silica 3 μm 4.6 x 150 mm column. Separations were monitored at 478 nm at room temperature. The flow was 1.2 mL/min with a total run time of 20 minutes. The mobile phase consisted of hexanes (solvent A) and acetone (solvent B) in an 82:18 ratio, under isocratic conditions.

For astaxanthin esters analysis, the samples were dissolved in 1 mL of mobile phase. All separations were monitored at 478 nm at room temperature. The flow was 0.85 mL/min. The

mobile phase consisted of hexanes (solvent A) and acetone (solvent B). The samples were initially eluted with 96 % A and 4 % B and augmenting B to 12 % over 20 min. The gradient changed to 18 % B during the next 10 minutes and brought back to initial conditions over 10 minutes. Equilibration time between runs was 10 minutes.³¹ Chiral separation of astaxanthin extracted from shrimp oil was performed using a Chiralpack IC 5 μm 4.6 x 250 mm column. Separations were monitored at 476 nm at room temperature under isocratic conditions. The mobile phase consisted of acetonitrile (solvent A) and methyl *tert*-butyl ether (solvent B) in a 1:1 ratio. The flow was 1 mL/min and total run time of 20 minutes.³²

Total fatty acid profile (TFAP) of shrimp oil was acquired using fatty acid methyl esters (FAME) analysis and was performed on a Varian 3900 GC-FID system. The separation was performed on a ZB-Wax capillary column 20m x 0.18mm x 0.18 μm . The oven was on gradient mode starting at 140°C for 0.2 min with a ramp to 170°C (40°C/min), ramp to 185°C (4°C/min) and finally ramp to 230°C (2°C/min). Data was processed using the Galaxy software. The method use for TFAP was adapted from the one developed by Lepage *et al.*³³

NMR

All NMR spectra were recorded on a Bruker Advance III 400 MHz. ^1H NMR chemical shifts are reported relative to TMS and were referenced via residual proton resonances of the appropriate deuterated solvent. Structures were validated using a combination of ^1H , $^{13}\text{C}\{^1\text{H}\}$ and 2D experiments.

FTIR

FTIR analysis was conducted on a Varian 640-IR spectrometer with a tungsten-halogen source, emission band lead selenide detector, and a single reflection MIRacle diamond crystal (PIKE technologies) of 2 mm diameter. The astaxanthin esters samples and shrimp oil samples were deposited on the crystal before scanning. A background scan was run previous to scanning the samples. Single beam spectra were obtained by averaging 32 scans with a 1.5 cm^{-1} resolution and a scan speed of 20 kHz.

Raman

For the Raman measurements, a drop of the collected fraction was deposited on a standard Drop Coating Deposition Raman (DCDR) substrate. After the solvent evaporation, ASTX esters were studied by a confocal high Resolution Raman microscope (Jobin-Yvon Labram HR) equipped with a motorized xy stage and autofocus. The Raman spectra were generated with a 17 mW, 632.8 nm wavelength, He-Ne laser excitation and dispersed with the 1800 grooves/mm grating across the 0.8 m length of the spectrograph at room temperature. The laser power was 4 mW at the sample surface, and the spectral resolution is estimated to be less than 0.5 cm^{-1} for a slit width of 150 μm and a confocal hole of 300 μm . In order to ascertain the findings, at least 5 spectra were recorded for each sample and were analysed. The laser power was reduced by 100 times

at the sample surface using an optical density filter to eliminate the possibility of laser induced damage to the ASTX-esters.

Conclusions

Astaxanthin-rich shrimp oil was recently discovered in the Acadian Peninsula region of Canada; it was extracted from the waters used in a shrimp processing plant. A compositional analysis was performed in order to identify the beneficial health components of this shrimp oil. The total fatty acid profile indicated almost 50% monounsaturated fatty acids, 22% polyunsaturated and 20% omega-3 fatty acids. Chromatographic analysis revealed that almost all the ASTX is present in esterified form, with 75 % as diesters. ASTX and its esters were isolated from the shrimp oil and studied for their molecular properties using NMR, FTIR and Raman analytical methods. In order to identify the ASTX mono/diesters, control compounds of ASTX monoester and diesters were synthesized. Esterification was performed with heneicosanoic acid (C21)(1), 9-octadecenoic acid (C18:1n-9)(2) and docosahexaenoic acid (DHA, C22:6n-3)(3), which resulted in the mono- (a) and the diester (b) as well as some unreacted free ASTX. FTIR analysis showed clearly distinguishable signatures of mono- and diesters of ASTX, as shown by the clear spectral shift of vibrational mode corresponding to C=O of ASTX β -ionone ring with esterified and non-esterified ends. Raman spectroscopy identified important intermolecular interactions among ASTX esters, as shown by the signature modes of head to tail interaction of ASTX monoesters and π -stacking modes of ASTX diesters.

These results were applied to the NMR, FTIR and Raman studies of astaxanthin-rich shrimp oil. Compositional analysis of the astaxanthin-rich shrimp oil has revealed the presence of health beneficial fatty acids, such as EPA, and DHA, along with significant quantities of astaxanthin. In addition, Raman spectroscopy allowed detection of ASTX in the ppm levels directly in astaxanthin-rich shrimp oil.

Acknowledgements

The financial support of the Atlantic Innovation Fund Round VI (Project # 193594), the Industrial R&D Post-doctoral Fellowship of National Science and Engineering Research Council (NSERC) of Canada, the John R. Evans Leaders Fund of Canada Foundation for Innovation (CFI), and the Research Technicians Initiative (RTI) of New Brunswick Innovation Fund (NBIF) are gratefully acknowledged.

Notes and references

- 1 I. Higuera-Ciapara, L. Féliz-Valenzuela and F. M. Goycoolea, *Cr. Rev. Food Sci.* 2000, **46**, 184.
- 2 P. Kidd, *Altern. Med. Rev.*, 2011, **16**, 355.
- 3 R. G. Fassett and J. S. Coombes, *Molecules*, 2012, **17**, 2030.

- 4 Y. Yang, B. Kim and J. Y. Lee, *Hum. Nutr. Food Sci.*, 2013, **1**, 1003.
- 5 J. S. Park, J. H. Chyun, Y. K. Kim, L. L. Line and B. P. Chew, *Nutr. Metab. (Lond)*, 2010, **7**, 1.
- 6 K. Nakagawa, T. Kiko, T. Miyazawa, G. Carpennero Burdeos, F. Kimura, A. Satoh and T. Miyazawa, *Br. J. Nutr.*, 2011, **105**, 1563.
- 7 A. Satoh, S. Tsuji, Y. Okada, N. Murakami, M. Urami, K. Nakagawa, M. Ishikura, M. Katagiri, Y. Koga and T. Shirasawa, *J. Clin. Biochem. Nutr.*, 2009, **44**, 280.
- 8 Roche Vitamins and Fine Chemicals. Astaxanthin as a pigmenter in salmon feed (1987). <http://www.fda.gov/ohrms/dockets/dockets/95s0316/95s-0316-rpt0237-11-Tab-I-vol172.pdf> [Accessed August 25, 2014]
- 9 S. Reagan-Shaw, M. Nihal and N. Ahmad, *FASEB J.*, 2008, **22**, 659.
- 10 B. Renstrom, G. Borch, O. Skulberg and S. Liaaen-Jensen, *Phytochem.*, 1981, **20**, 2561.
- 11 B. Renstrom and S. Liaaen-Jensen, *Comp. Biochem. Physiol.*, 1981, **B69**, 625.
- 12 K. Holtin, M. Kuehnle, J. Rehbein, P. Schuler, G. Nicholson and K. Albert, *Anal. Bioanal. Chem.*, 2009, **395**, 1613.
- 13 D. E. Breithaupt, *J. Agric. Food Chem.*, 2004, **52**, 3870.
- 14 S. Takaichi, K. Matsuib, M. Nakamura, M. Muramatsuc and S. Hanadac, *Comp. Biochem. Physiol. B*, 2003, **136**, 317.
- 15 M. D. Grynbaum, P. Hentschel, K. Putzbach, J. Rehbein, M. Krucker, G. Nicholson and K. Albert, *J. Sep. Sci.*, 2005, **28**, 1685.
- 16 A. Guillou, M. Khalil and L. Adambounou, *Aquaculture*, 1995, **130**, 351.
- 17 H. Rajasingh, L. Øyehaug, D. I. Våge and S. W. Omholt, *BMC Biol.*, 2006, **4**, 10.
- 18 A. R. Rao, H. N. Sindhuja, M. D. Shylaja, K. U. Sankar, R. Sarada and G. A. Ravishankar, *J. Agric. Food Chem.*, 2013, **61**, 3842.
- 19 N. Tchoukanova and G. Benoit, Procédé d'extraction de solides organiques et d'huile d'organismes marins enrichis en astaxanthine. *WO PCT*, 2014138920 A1, 2014.
- 20 G. Jiao, J. P. M. Hui, I. W. Burton, M.-H. Thibault, C. Pelletier, J. Boudreau, N. Tchoukanova, B. Subramanian, Y. Djaoued, H. S. Ewart, J. Gagnon, K. V. Ewart and J. Zhang, *Mar. Drugs*, 2015, **13**, 3849.
- 21 H. Fukami, K. Namikawa, N. Sugiura-Tomimori, M. Sumida, K. Katano and M. Nakao, *J. Oleo Sci.*, 2006, **55**, 653.
- 22 H. Kobayashi, M. Yoshida, I. Maeda and K. Myashita, *J. Oleo Sci.*, 2004, **53**, 105.
- 23 C. Yuan, Z. Jin and X. Xu, *Carbohydr. Polym.*, 2012, **89**, 492.
- 24 F. J. G. Muriana, V. Ruiz-Gutierrez, M. L. Gallardo-Guerrero and M. I. Minguez-Mosquera, *J. Biochem.*, 1993, **114**, 223.
- 25 B. Subramanian, N. Tchoukanova, Y. Djaoued, C. Pelletier, M. Ferron and J. Robichaud, *J. Raman Spectrosc.*, 2014, **45**, 299.
- 26 B. Subramanian, N. Tchoukanova, Y. Djaoued, C. Pelletier and M. Ferron, *J. Raman Spectrosc.*, 2013, **44**, 219.
- 27 S. Yoshida and H. Yoshida, *Biopolymers*, 2003, **70**, 604.
- 28 Y. Miyake, K. Yokomizo and N. Matsuzaki, *J. Am. Oil Chem. Soc.*, 1998, **75**, 1091.
- 29 M. D. Guillén and A. Ruiz, *Trends Food Sci. Tech.*, 2002, **12**, 328.
- 30 R. Sacchi, F. Addeo and L. Paolillo, *Magn. Reson. Chem.*, 1997, **35**, S133.
- 31 Addapted from: Lorenz RT (2001) BioAstin/NatuRose TM Technical Bulletin #017. Cyanotech Corporation
- 32 C. Wang, D. W. Armstrong, and C.-D. Chang, *J. Chromatogr. A*, 2008, **1194**, 172.
- 33 G. Lepage and C. C. Roy, *J. Lipids Res.*, 1984, **25**, 1391.